Effects of ullage height on heat feedback and combustion emission mechanisms of heptane pool fires

Liu, Chunxiang; Ding, Long; Jangi, Mehdi; Ji, Jie; Yu, Longxing

DOI:
10.1016/j.firesaf.2021.103401

Document Version
Peer reviewed version

Citation for published version (Harvard):
Liu, C, Ding, L, Jangi, M, Ji, J & Yu, L 2021, 'Effects of ullage height on heat feedback and combustion emission mechanisms of heptane pool fires', *Fire Safety Journal*, vol. 124, 103401.
https://doi.org/10.1016/j.firesaf.2021.103401

Effects of ullage height on heat feedback and combustion emission mechanisms of heptane pool fires

Chunxiang Liu [a], Long Ding [a], Mehdi Jangi [b], Jie Ji [a,*], Longxing Yu [a]

[a] *State Key Laboratory of Fire Science, University of Science and Technology of China, JinZhai Road 96, Hefei, Anhui 230026, China*

[b] *School of Mechanical Engineering, University of Birmingham, Edgbaston, Birmingham B15 2TT, UK*

Corresponding Author: **Jie Ji (Prof. & Ph. D)**, State Key Laboratory of Fire Science, University of Science and Technology of China, Hefei, Anhui 230026, China.

Tel.: +86 0551 63606431; Fax: +86 551 63606430; Email: jijie232@ustc.edu.cn.

Abstract

This paper investigates the effects of ullage height (distance between the fuel surface and the pool upper rim) on heat feedback and combustion emission mechanisms of heptane pool fires. Results showed that ullage height significantly influences the flame structure and fuel mass loss rate. The incident radiative heat flux to the fuel surface and its heat feedback fraction first increase and then decrease with ullage height. Correspondingly, the convective heat feedback fraction presents a reverse trend. This attributes to flame base suspension effect and the evolution of soot volume fraction of the flame due to incomplete combustion. While for the conductive heat feedback fraction, it increases with ullage height and becomes the dominant heat feedback mode when the ullage height increases to a certain value. The profiles of the generation rate of the smoke particulates well explain the evolutions of the incident radiative heat flux. The combustion completeness is characterized by the ratio of CO/CO_2. Furthermore, it is calculated that the maximum combustion completeness decreases by 18.4 % and 14.3 % for pool diameters of 10 cm and 15 cm, respectively. These findings will help to develop

and establish more general heat transfer and heat release rate models for pool fires.

Keywords: pool fire, ullage height, heat feedback, combustion emission, mass loss rate, combustion completeness

1. Introduction

Pool fires are widely used as the energy release source to simulate fire occurrence and development in scientific research and engineering applications. For example, pool fire is often applied to study the heat transfer and combustion behaviors in tunnel [1] and high-rise buildings [2]. Based on the pool fire theories of fire plume and heat release rate, regulations of fire protection design and safety evacuation have been developed as mandatory standards.

For pool fires, heat feedback to the fuel includes conductive heat flux from the pool sidewall, and convective and radiative heat flux from the flame. Previous studies pointed out that, depending on the pool diameter and the turbulent regime of the flame, the dominant heat transfer mechanisms for pool fires could be classified into [3, 4]: conduction for laminar flame with $D < 0.03$ m; convection for turbulent flame with 0.03 m $\leq D <$ 1.0 m; and radiation for turbulent flame with $D \geq$ 1.0 m. Hamins et al. [5] investigated the radial variation of heat feedback of pool fires with a diameter of 0.3 m. They found that the variation of radiative heat feedback along the fuel surface is generally identical for fuels with a luminous flame. Nakakuki [6] analyzed the effects of wall materials and thickness on the heat transfer mechanisms of small-scale pool fires. It was found that heat transferred from the flame to the pool sidewall and then transferred convectively to the liquid was the dominant heat feedback. Zhao et al. [7] measured the heat feedback of thin-layer pool fires and pointed that the heat flux feedback from the flame remains almost constant except for the igniting and extinguishing periods. Kuang [8] studied the effects of cross air flow on flame radiative feedback of pool fires. They concluded that the radiative feedback reduced to a constant value as cross air flow increased. Ge et al. [9] studied the evolution of heat feedback in

multiple pool fires and found that heat feedback was influenced by the flame characteristics and the burning behaviors. Wan et al. [10] investigated the heat back mechanism of two unequal circular pool fires and summarized that, for a given target pool fire, heat feedback fractions were weakly affected by the adjacent pool fire scale.

It should be noted that the above conclusions are deduced from near zero ullage height conditions. However, under the effect of pool ullage, the burning behaviors of pool fire will be more complicated than that of the zero ullage height conditions. Apparently, the flames characteristics and the mass loss rate are significantly changed under different ullage height conditions. For example, Blinov and Khudyakov [11] revealed that the flame oscillation behaviors of pool fires were sensitive to the fuel level depth (ullage height), and the flame started to enter into the pool under certain ullage height conditions. Oraff [12] found out that the PMMA flame shape became more turbulent and thicker as the container ullage height increased, resulting in the change of flame radiation properties. Dlugogorski and Walson [13] studied the effects of ullage height on fuel mass loss rate and analyzed the evolutions of flame characteristics. More recently, Shi et al. [14] experimentally and numerically studied the ullage height effect on burning behavior of small scale (D =2.5 cm, 5 cm) methanol pool fires. They found out that the flame initially anchored around the pool rim under small ullage height conditions, and then it partially covered the burner due to the plume axial flapping as the ullage height grew large. Liu et al. [15-17] conducted experimental and numerical studies focusing on the effects of ullage height on the flame characteristics, plume centerline temperature, and plume flow and combustion characteristics.

Based on the aforementioned works, we can conclude that the existence of ullage height will change the flame characteristics, including flame turbulence enhancements, the flame oscillation behavior, the entering of flame base into the pool, and so on. Then, heat feedback mechanisms would also be affected. These effects can result from the changes of : (I) conductive heat transfer from the pool sidewall to the fuel, especially when the flame enters into the pool and the pool diameter is small; (II) convective heat transfer between the flame base and the fuel surface, which is caused by the flame base

turbulence being altered when the flame base detaches from the fuel surface at minor ullage height and when it enters into the pool at large ullage height; (III) radiative heat feedback, since the flame thickness and flame shape are sensitive to the ullage height.

Till now, there still remains a research gap in the effects of ullage height on the heat feedback mechanisms of pool fires. How exactly the heat feedback mechanisms (conduction, convection, and radiation) are changed as the ullage height increases, are still unknown. Besides, the evolution of the combustion completeness under the influence of ullage height is also not available in the current literature. Instead, empirical data obtained from near zero ullage height conditions are often adopted, which brings uncertainties for the management and design of fire safety.

In this paper, a set of experimental apparatuses were designed, with the flame shape, mass loss rate, the temperatures of the pool sidewall and the liquid fuel, the incident radiative heat flux on the fuel surface, and the combustion emission products (smoke particulates, CO, CO_2) being systematically measured and analyzed. This study will help to understand the heat feedback and combustion emission mechanisms of pool fires under the influence of ullage height. Moreover, it has the potential to set up a more practical model to predict the mass loss rate (or heat release rate) when the ullage height is non-zero in a real fire.

2. Experimental setup

2.1 Measurement of the combustion emission products

Figure 1 shows the schematic of the experimental setup. Figure 1(a) is the combustion emission test system which follows the ASTM E2058 standards [18]. The combustion emission products are exhausted and mixed well in the mixing duct. In the measuring duct, a thermocouple is inserted into the center of the duct to measure the gas temperature with an accuracy of 1.0 ^{o}C. The mass flow rate of the gas stream in the duct is measured by the averaging Pitot probe, based on the pressure differential. The gas sampling probe, connecting to a soot filter, moisture remover system and other facilities, is used to measure the volume fraction of CO, CO_2 and O_2. The smoke particulates were

measured in the smoke duct through a laser system, based on the smoke extinction method. The detailed formulas are presented in section 3.4. To have a good comparison, each test was conducted with the same initial temperature and lasted long enough to reach its steady-burning stage from which the experimental data of more than 200 s was intercepted for analysis.

2.2 Experimental pools

Figure 1(b) shows the schematic of the designed experimental pool. During experiments, the fuel level in the pool was maintained at a constant height by a fuel level maintaining device (Fig. 1(b1)). The fuel level maintaining device was placed on an electronic balance to record the instantaneous mass losses during experiments. The maximum load of the balance is 34 kg, with an accuracy of 0.01 g and the sampling frequency of 1 Hz. Two fuel pools were used during experiments, with internal diameters of 10 cm and 15 cm. The fuel pools are made of stainless steel, with a thickness of 5 mm and an internal depth of 45 mm. A series of hollow cylinders with different heights (h) are made and tightly wedged on the pool to obtain different ullage heights. The hollow cylinders are made of the same material, and have the same thickness and diameter as the corresponding pool. h was changed from zero to the value that the fire self-extinguished. For the two pools, non-dimensional ullage height (h/D) was set as 0, 0.1, 0.2, 0.3, 0.4, 0.5, 0.6, 0.7, 0.8, 0.9, 1.0, 1.2, 1.4. Two HD cameras were used to record the flame shape, with a spatial resolution of 1920 x 1080 and the frame rate of 50 fps. One was placed straight ahead of the pool of 150 cm to record the whole evolution of flame shape outside of the pool. The other one was placed near the pool of 50 cm to record the detailed flame behaviors near the pool upper rim. All tests were repeated at least three times, the detailed experimental and model errors were evaluated in the appendix.

2.3 Measurement of heat feedback

2.3.1 Conductive heat feedback

The conductive heat flux conducted between the pool sidewall and the fuel is the

result of the temperature difference between them. While in the current study, there are temperature gradients for the pool sidewall and the fuel in the vertical direction. Nakakuki [6] studied the conductive heat transfer mechanism between pool sidewall and the fuel and pointed out that the pool sidewall temperature (T_w) and its nearby fuel temperature (T_l) could be respectively estimated at 0.5 L (L is the fuel thickness) and 0.2 L (Fig. 1(b3)). The credibility of this conclusion has been widely proved in the heat transfer analysis of pool fires with different boundary conditions [9, 10, 19]. In the current study, the heat transfer mechanisms between the pool sidewall and the fuel is not changed by the ullage height. Thus, we applied this relationship to analyze the conductive heat feedback. As shown in Fig. 1(b3), T_l was placed within the fuel with 10 mm horizontally away from the pool inner sidewall, and T_w was embedded in the middle of the pool sidewall. Thermocouples applied in the current study were K-type, with a diameter of 1 mm. The response time (time to react to a sudden temperature variation) of the thermocouples was less than 1 s. And, the analyzed pool sidewall and the fuel temperatures were averaged from data of more than 200 s, intercepted from the steady-burning stage, which is adequate for measuring the stable temperature field. The credibility of this method have been widely recognized [20-22]. N-heptane (boiling point: 98℃) was used as the experimental fuel.

2.3.2 Radiative heat feedback

The measurement of radiative heat feedback received by the fuel surface based on the assumption that radiative heat feedback on the fuel surface is uniform. Hamins et al. [5] investigated the radial variation of heat feedback of pool fires with a diameter of 0.3 m. They found that the variation of radiative heat feedback along the fuel surface was generally identical for fuels (heptane, toluene) with a luminous flame. Ma et al. [23] conducted numerical studies about the effects of pool boundary conditions on pool fires. According to their numerical results, radial radiative heat feedback was essentially identical along the fuel surface. Thus, to minimize the effect of the radiometer installation on the combustion process, a water-cooled radiometer protected by a quartz glass hood was placed on the fuel surface to record the incident radiative heat flux.

Luketa [24] compared the burning mass flux of pool fires with and without crushed glass and concluded that there was little difference. Then, it is anticipated that the influences of the quartz hood are acceptable. A similar method was also applied by previous studies [4, 9, 10]. The external diameter of the quartz hood was 20 mm. Area ratios of the radiometer to the fuel surface are 4.0 % (D= 10 cm) and 1.8 % (D = 15 cm). In the pre-experiment, we have compared the burning rate of with and without radiometer and found that the influence of radiometer on the burning rate was insignificant. The radiometer was placed on the pool middle to achieve a better view angle for the radiation measurement. The quartz glass hood has a thickness of 3 mm. The maximum measuring range of the radiometer is 10 kW/ m^2, and the viewing angle is 150°. Highly transparent quartz hood was used to minimize its blockage effect on the flame radiation. And, before each test, we carefully polished the hood with alcoholic cotton to eliminate soot deposition. Between the flame base and the fuel surface, there are radiative, convective, and conductive heat transfer. Apart from protecting the radiometer, the highly transparent glass hood also filtered the convective and conductive heat flux to make sure the radiative heat flux was measured separately [10]. The transmissivity of the quartz hood, α, was obtained by, $\alpha = I / I_r$, where I and I_r were the measured radiative heat flux intensity with and without quartz hood. The detailed formulas about the calculations of conductive and radiative heat flux are presented in section 3.3.

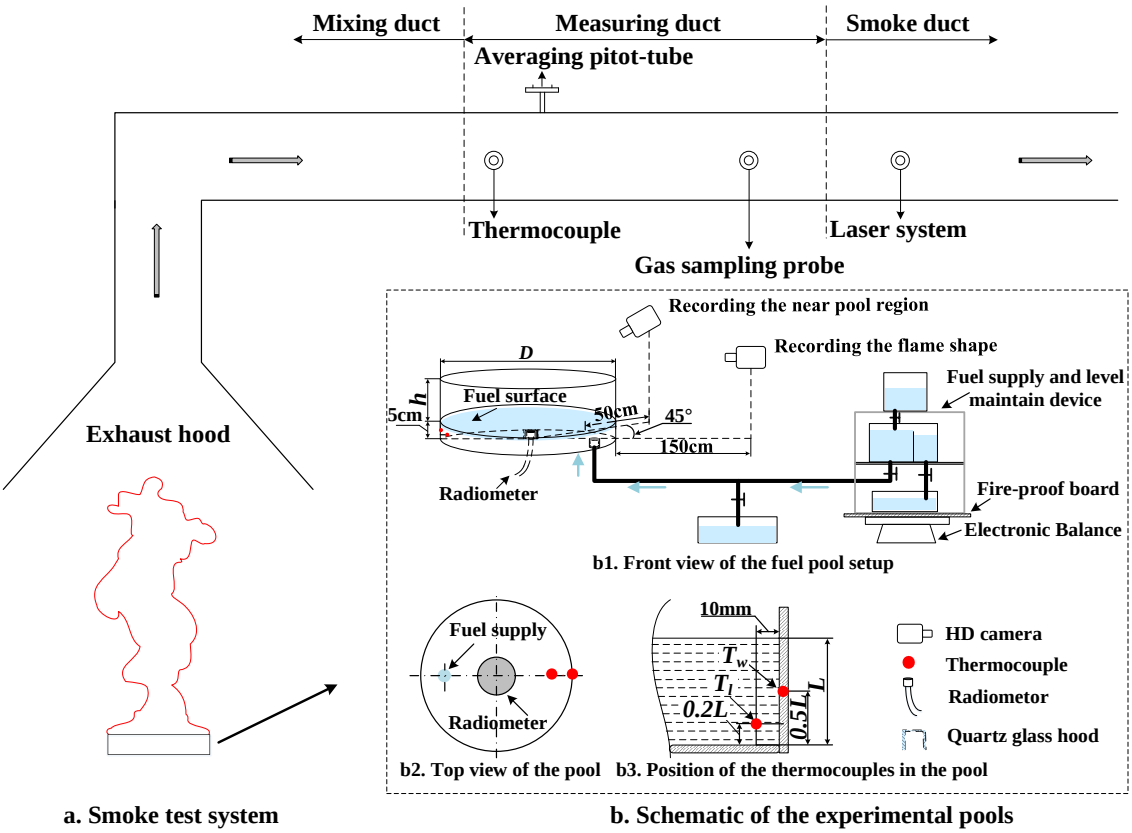

Fig. 1. Experimental setup.

3. Results and discussion

3.1 Flame shape

Figure 2 shows the experimental photos of typical ullage height conditions, shot from straight ahead and close range of the pool. When h/D=0, the fuel vapor evaporates from the fuel surface and freely mixes with the ambient air. An intermittent fire plume develops at a height of about 10 cm above the fuel surface. Under the effect of ullage height (h/D=0.1, 0.3, 0.6), the flame shape is like a rising mushroom cloud. Besides, the unstable fire plume begins to form near the ullage upper rim, and then it rolls upward, with the beneath plume showing a necking-in behavior. According to experimental observations, the outside plume was getting more stable under higher ullage height conditions (h/D=1.0, 1.4), with the flame moving less in vertical and horizontal directions. However, near the pool outlet, the flame was growing turbulent, which resulted from the movements of surrounding air entrained into the pool, mixing with

the fuel gas, and combusting within the pool. And, the luminous part of the flame base did not extend to cover all over the pool, but it kept a certain distance from the part of the rim wall leaving a non-flame region around the pool mouth. Near the non-flame region, it was observed that the flame flowed inside the pool indicating a path of the ambient air entrained into the pool. After that, the air would mix with the fuel vapor inside the pool, and the fire plume left the pool from the other parts of the pool mouth. Nonetheless, it was seen that at a higher h/D, the luminous part of the flame base was getting smaller and was limited within the interior part of the pool surface. This might imply the changes of heat transfer from the flame to the pool ullage then conducted to the fuel, or changes of directly radiative and convective heat transfer from the flame to the fuel surface.

We calculated the flame pulsation frequency in Fig. 2, based on the Fast Fourier Transformation (FFT) method [25-27]. It shows that the flame pulsation frequency decreases with the increase of ullage height for 15-cm pool fires, and a similar trend was also found for 10-cm pool fires with flame pulsation frequency decreasing from 5.26 Hz (h/D=0) to 2.83 Hz (h/D=1.4). The decreased flame oscillation frequency results from the enhanced air entrainment restriction, which significantly affects the initiation and formation of the vortical toroidal structure near the flame base and its following upward development. Studies conducted by Weckman et al. [28], Rangwala et al. [29], and Fang et al. [30] have revealed similar behaviors. Weckman et al. [28] enclosed the pool with different screen fences to disturb the flow of air into the flame. They found that, under the effects of the fence, ribs and channels were evident near the flame base and growing sharper with longer fences. Rangwala et al. [29], and Fang et al. [30] investigated the effects of immersed obstacles on the burning behaviors of pool fires. They found that the flame height was significantly stretched to entrain more air. Our study and the above literatures demonstrate that the changed flame structure was caused by the disturbed air entrainment.

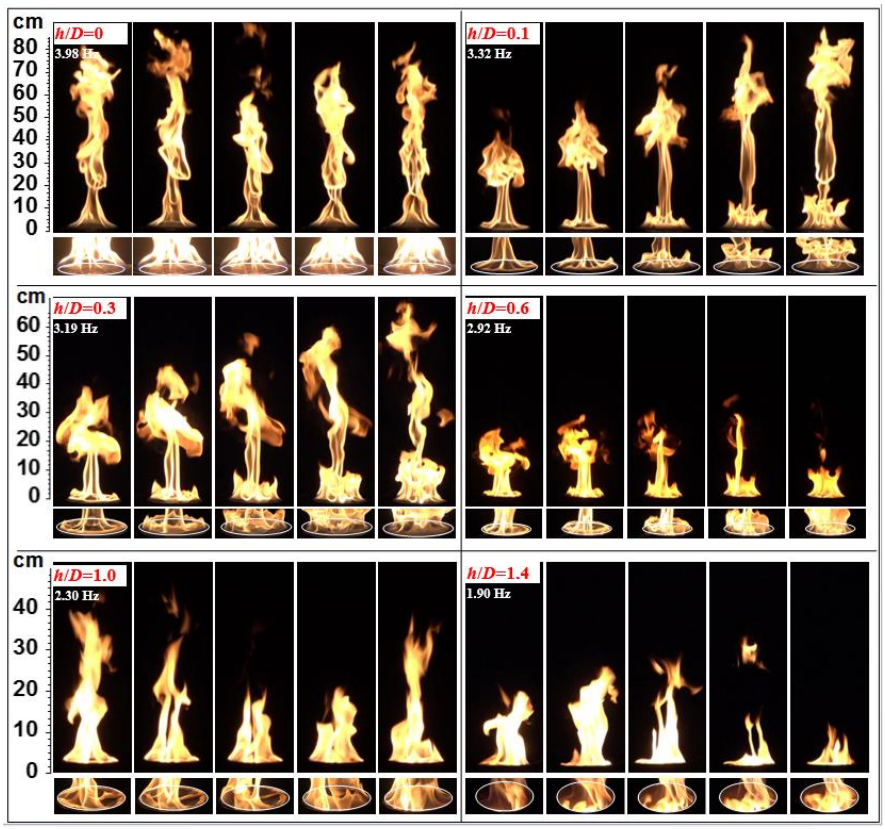

Fig. 2 Typical time-sequential experimental snapshots under different non-dimensional ullage height *h*/*D* with *D* =15 cm.

3.2 Mass loss rate

Mass loss rate, m', of classic pool fires (with zero or near-zero ullage height) can be classified into three regimes [3, 4], namely, I. laminar regime, with m' falling with D (D < 0.03 m), II. transitional regime (0.03 m < D < 1 m), III. turbulent regime, with m' becoming independent of D (D > 1 m). In transitional and turbulent regimes, correlation between m' and D was given [3],

$$m' = m'_{\infty}(1-e^{-\kappa\beta D}) \tag{1}$$

where κ is the absorption-extinction coefficient of the flame, β is a mean beam length corrector. m'_{∞} is the mass loss rate for pool fires with unlimited diameter. The values for m'_{∞}, κ, and β can be referred in literatures [3, 32]. Figure 3 shows the mass loss rate in all cases. As shown in Fig. 3, the credibility of the current study has been well confirmed through comparing with literature data [8, 33, 34] of near-zero

ullage height conditions. And, it can be observed from Fig. 3 that generally the mass loss rate decreases with the increase of the ullage height, which indicates less heat feedback to the liquid fuel. Model predictions of Eq. (1) are also shown in Fig. 3, which demonstrates that classic model is only applicable to those with minor ullage height (h/D) conditions. The deviations between model predictions and the experimental results increase with h/D. Basically, two competing effects that influence the burning rate, i.e. enhanced conductive heat flux transferred from the flame to the pool ullage then transferred to the fuel through adjacent pool sidewall, and increased air entrainment restriction. Experimental results demonstrated in Fig. 3 imply that for the given target pool fires the burning rate is mainly influenced by the air entrainment restriction.

The average temperatures of the pool sidewall and the liquid fuel of all cases are shown in Fig. 4. From Fig. 4, the average temperatures of the pool sidewall (T_w) and the liquid fuel (T_l) slightly increase with pool diameter. Under the same diameter, T_w and T_l remain also constant as h/D increases. And, the temperature differences ($\triangle T$) between T_w and T_l are nearly unchanged in all cases. It is anticipated that there are two competing effects between the enhanced feedback of more heat transferred to the fuel and the pool sidewall as more flame burning occurs inside the pool, and the increased heat loss from the increased sidewall area. This means that conductive heat flux from the pool wall to the fuel is nearly not changed for the pool with the same diameter, since the conductive heat flux in pool fires is determined by ΔT and the contacting area [9, 11]. The effects of ullage height on mass loss rate would then mainly influence the other two parts (radiative and convective) heat transfer mechanisms. According to Fig. 2, the flame characteristics (flame turbulence and flame distribution near the pool mouth) are sensitive to the ullage height. Then, the mixing process of the entrained air and the fuel vapor, and the convective heat transfer coefficient between the flame base and the fuel surface might be changed. It is therefore needed to characterize the evolutions of radiative and convective heat feedback under various ullage height conditions.

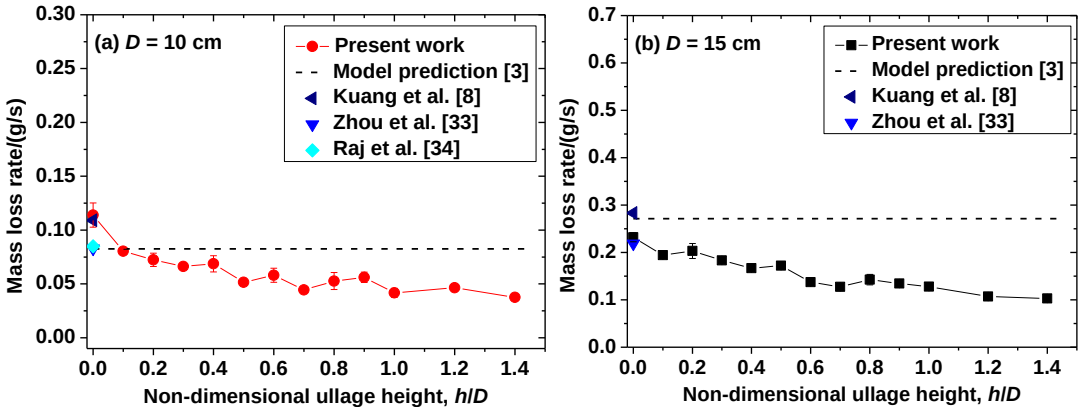

Fig. 3. Mass loss rate under different ullage height conditions.

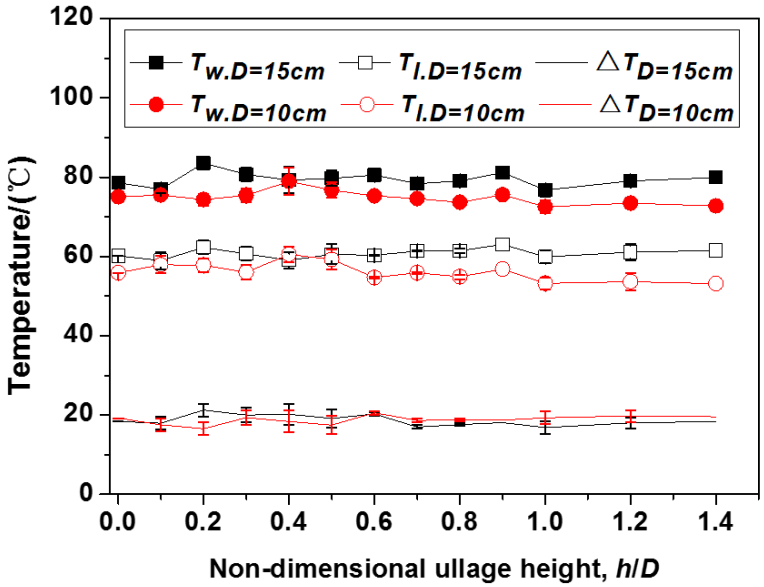

Fig. 4. Average pool sidewall (T_w) and liquid fuel (T_l) temperatures of steady stage.

3.3 Heat feedback

Figure 5 demonstrates the heat balance of the liquid fuel during steady burning stages after it was ignited about 1800 s. As shown in Fig. 5, considering the fuel as the control volume, heat received (input) by the liquid fuel includes the conductive heat feedback from the contacting pool sidewall, $Q_{cond.,w}$, the radiative heat feedback from the flame, $Q_{rad.,f}$, and the convective heat feedback between the plume base and the fuel surface, $Q_{conv.,f}$. Heat output mainly consists of the heat to heat the fuel and then evaporates it from the fuel surface, $Q_{fuel.}$, the re-radiation from the liquid fuel to the surroundings, $Q_{re-rad.,l}$, and the heat loss to the bottom supplying cold fuel and then

through bottom pool sidewall to the environment, $Q_{loss,l}$. Therefore, the fuel heat balance is expressed as,

$$Q_{fuel} + Q_{re-rad.,l} + Q_{loss,l} = Q_{rad.,f} + Q_{cond.,w} + Q_{conv.,f} \quad (2)$$

According to the study of Hamins et al. [32], $Q_{re-rad.,l}$ and $Q_{loss,l}$, are typically small when compared with Q_{fuel} for liquid fuels, thus could be neglected. According to experimental observations, the fuel boils at stable stage, thus Q_{fuel} could be calculated as,

$$Q_{fuel} = m'[H_v + c_p(T_{boil} - T_o)] \quad (3)$$

where m' is the mass loss rate, H_v is the heptane evaporation heat, c_p is the heptane specific heat, T_{boil} and T_o respectively represent the boiling point of heptane and the initial fuel temperature.

The radiative heat feedback, $Q_{rad.,f}$, is calculated based on the measured incident radiative heat flux per unit area multiplied by the fuel surface area, which can be expressed as follows.

$$Q_{rad.,f} = \pi\tau D^2 q_{rad.} / 4 \quad (4)$$

where τ is the transmissivity of the quartz hood covered over the radiometer, and is calibrated by the heat flux of heptane flame during each test. D is the diameter of the fuel surface, $q_{rad.}$ is the measured incident radiative heat flux per unit area. Figure 6 shows the measured incident radiative heat flux of all cases. From Fig. 6, it can be seen that the incident radiative heat flux increases first and then decrease with the ullage height. This trend might be explained by the soot volume fractions of the flame base. As shown by the illustrations in Fig. 6, under zero ullage height conditions, the flame base tends to be blue and transparent. This is because the air is freely entrained into the plume and well mixed with the heptane vapor, then the soot in the flame produced due to incomplete combustion is small. Under minor ullage height conditions, the ullage would affect the transport of fuel vapor out of the pool and depress the mixing process

of the air and the fuel vapor. As a result, the flame tends to be thick and much more emissive. In this stage, the incident radiative heat flux shows an increasing trend. While as the ullage height becomes larger, the flame tends to be stubbier and sparse owing to its strong inhibition effect on the air entrainment. This makes the incident radiative heat flux tend to decrease.

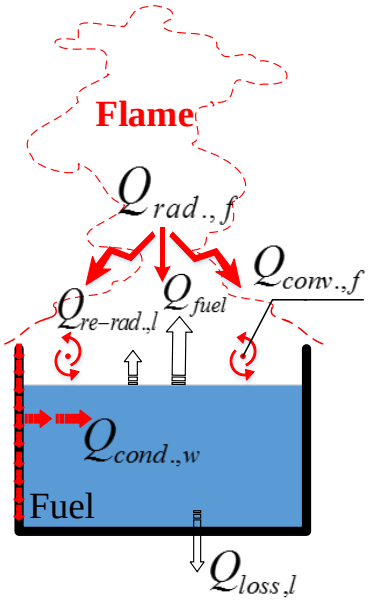

Fig. 5. Schematic of heat transfer to the fuel.

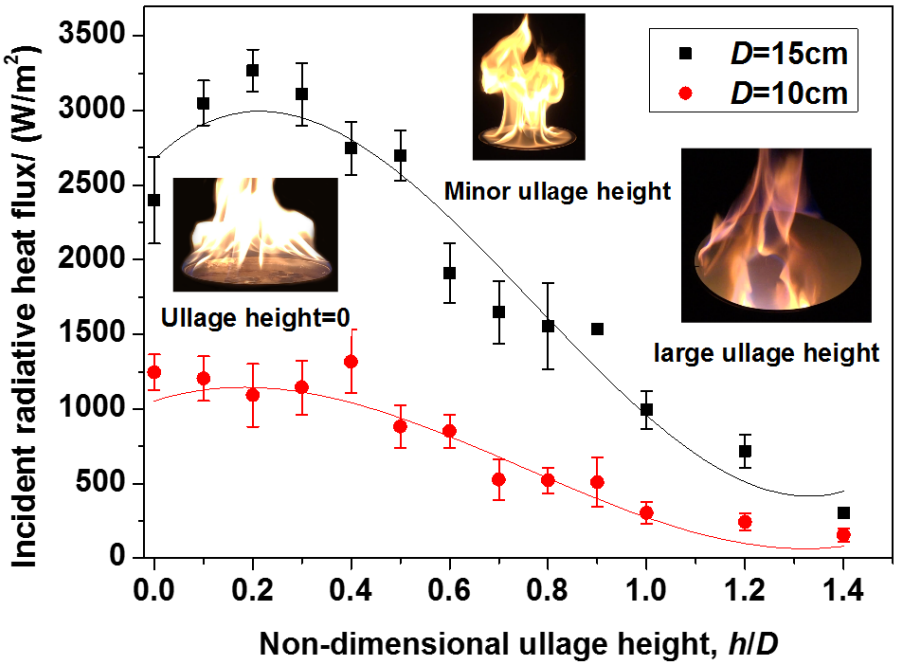

Fig. 6. Incident radiative heat flux on the fuel surface.

We further examined the heat transfer mechanisms by analyzing the heat transfer

budget of conduction, convection, and radiation in each case. The conductive heat feedback, $Q_{cond.,w}$, is a coupled conduction and convection heat transferred to the fuel via the pool sidewall. Previous studies have found that during the steady burning stage, there are two counter-rotating vortices adjacent to the pool sidewall due to the continuous fuel supply from the pool bottom by the fuel level maintainer devices [35]. And, thermal convective boundary layer theory [36] could be applied to calculate the heat transfer between the pool sidewall and the liquid fuel as follows.

$$Q_{cond.,w} = h(T_w - T_l)\pi DL \tag{5}$$

where T_w and T_l are the temperatures of the pool sidewall and the liquid fuel. L is the length of the convection layer and is estimated as the fuel thickness [6, 10, 19]. h is the average heat transfer coefficient and is obtained by,

$$Nu = hL / \lambda \tag{6}$$

where Nu is the Nusselt Number, λ is the thermal conductivity of the fuel. h could be reformulated as [6],

$$h = 0.502\lambda[(\frac{\mathrm{Pr}}{\mathrm{Pr}+\mathrm{Pr}^{1/2}+0.5})\frac{g\beta}{\alpha\upsilon L}]^{1/4}\cdot(T_w - T_l)^{1/4} \tag{7}$$

where Pr is the Prandtl Number, g is the gravity acceleration. β, α and υ are the thermal expansion coefficient, thermal diffusivity and kinematic viscosity of the liquid fuel. It should be noted that for all the above thermo-physical parameters, the values at the boundary layer temperature $((T_w + T_l)/2)$ are used. Then the heat feedback fraction for conduction ($\chi_{cond.}$), radiation ($\chi_{rad.}$), and convection ($\chi_{conv.}$) could be obtained as follows.

$$\chi_{cond.} = Q_{cond.,w} / Q_{fuel},\ \chi_{rad.} = Q_{rad.,f} / Q_{fuel},\ \chi_{conv.} = 1 - \chi_{cond.} - \chi_{rad.} \tag{8}$$

Figure 7 shows the variation of heat feedback fractions versus non-dimensional ullage height, h/D. It can be seen in Fig. 7 that $\chi_{cond.}$ is a monotonically increasing function of h/D, with a maximum value of approximately 0.6 for the current study. More importantly, the results show that conduction is the dominant heat transfer mode at large

ullage height conditions (for D=10 cm, $h/D \geq 0.5$; D =15 cm, h/D >1). It is known that using fire-fighting foams is one of the most popular ways to extinguish storage tank fires [37, 38]. However, historical data shows that the success rate of fire extinguishment is rather low [37]. This is due to the fact that, under intense temperature, the foam would evaporate, decompose, hardly disperse well on the burning fuel surface. Practically, weakening the fire growth and burning intensity is an applicable way for thermal hazard control and risk management. Figure 7 inspires that, for those pool fires with significant ullage height, cooling down the ullage wall temperature would be a reasonable way to weakening the fire growth and burning intensity. Despite $\chi_{rad.}$ initially increases and then decreases with h/D, for D = 15 cm, it is much less sensitive to the h/D at a smaller diameter of D = 10 cm. $\chi_{conv.}$ shows an opposite trend. The trend for $\chi_{rad.}$ is in accordance with the evolution of incident radiative heat flux as shown in Fig. 6, which is relevant to the evolution of the flame soot volume fraction. To avoid repetition, please refer to the discussion of Fig. 6. While for $\chi_{conv.}$, the initial decrease might be the result of flame suspension (flame base detaching from the fuel surface). It has been found that under minor ullage height conditions, the flame base would anchor around the pool upper rim [14]. Between the flame base and the fuel surface, it is filled with low turbulent fuel vapor. Thus, the convective heat feedback to the fuel surface would decrease in this stage. As the ullage height further increases, the flame base would enter into the pool which then enhances the plume turbulence intensities near the fuel surface, resulting in the growth of $\chi_{conv.}$.

Based on pool diameter, previous studies [3] classified the dominated heat feedback of pool fires into, conduction, convection, and radiation. For conductive heat feedback dominated pool fires, laminar flame was found. In this stage, the plume flow rate is low and soot is mainly released at the flame tip [3], which makes the convective and radiative heat feedback relatively insignificant. The plume flow rate increases with the pool diameter, resulting in the flame behaving more turbulent and more incandescent carbonaceous particles formed in the flame. The convective and radiative

heat feedback play an important role. However, as shown by the time-sequential snapshots in Fig. 2, nearly all the flames of different ullage heights demonstrate turbulent characteristics. The evolution of heat feedback is the coupling effects of air entrainment, plume turbulence, and mixing behaviors of fuel vapor and the entrained air, which in the end leads to changed combustion characteristics. Based on the combustion emission, the combustion behaviors of pool fires under the effects of ullage height are discussed below.

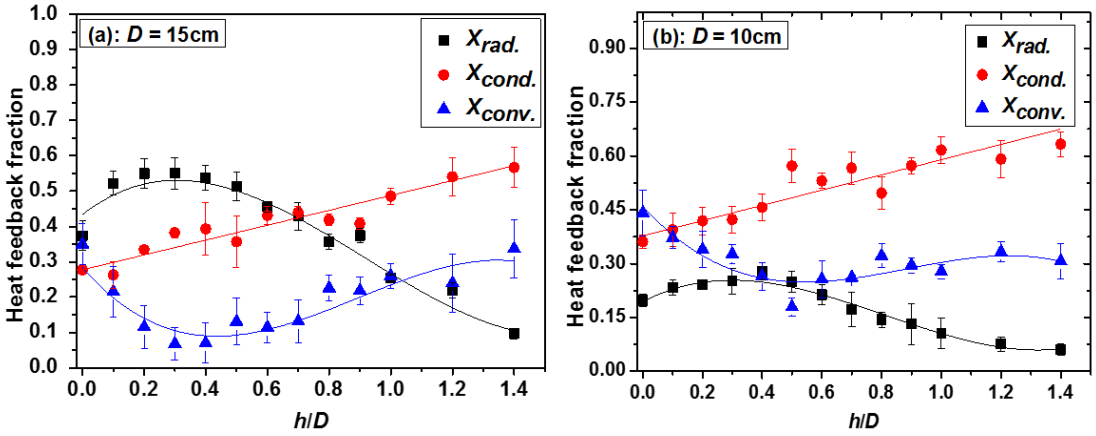

Fig. 7. Heat feedback fraction under different ullage height conditions.

3.4 Combustion emission products

Combustion emission products are important to characterize the energy conversion and pollutant emission. In fires, combustion emission products are released as a result of the fuel gasification, decomposition, and chemical reaction with the oxidizer. Specifically, the generation of the combustion emission products occurs in two zones [39], reduction zone and the oxidation zone. Soot, CO, hydrocarbons and other intermediate products are generated in the reduction zone. In the oxidation zone, the above products react with the oxidizer to form CO_2, H_2O, smoke particulates, and other products. Their reaction completeness and the following combustion emission products release depend on [39], the concentrations of the reduction products relative to the oxidizer, their temperature, and their mixing properties. In this study the combustion emission is affected by the ullage height due to its inhibition effect on the plume flow and mixing processes.

Soot is the dominant source that emits thermal radiation within the hydrocarbon flame [40], compared with CO, CO_2, and H_2O. Smoke particulates are generated due to a stop of the soot burnout, which is caused by the low temperature brought by the soot radiation losses [41]. Usually, the higher the soot volume fraction in the flame, the more smoke particulates will be generated. Therefore, the generation rate of the smoke particulates is used to indirectly reflect the evolution of the flame soot volume fraction. In this study, the generation rate of the smoke particulates (Y_s) is calculated based on the smoke extinction effect, and given as [42],

$$Y_s = m_s / m' \tag{9}$$

$$m_s = f_s V \rho_s / A \tag{10}$$

$$f_s = D' \lambda \times 10^{-6} / \Omega \tag{11}$$

$$D' = \ln(I_o / I) / l \tag{12}$$

where m_s is the mass generation of the smoke particulates, m' is the fuel consumption, f_s is the smoke volume fraction, V is the volume flow rate in the exhaust system, ρ_s is the smoke density, A is the burning area, λ is the wavelength of the light source , Ω is the smoke extinction coefficient, D' is the optical density, I_o / I is the fraction of monochromatic light transmitted through smoke, l is the optical path length.

Figure 8 shows the variations of the nominalized generation rate of the smoke particulates under different *h*/*D*. It can be concluded that the generation rate firstly increases then decreases with *h*/*D*, which implies that soot generation in the reduction zone also firstly increases then decreases as *h*/*D* increases. This, to some extent, explained the trend of the incident radiative heat flux received by the fuel surface (Fig. 6). Besides, Fig. 8 also indicates that more smoke particulates are generated per unit mass of fuel in pool fires with a bigger diameter. The higher generation rate of the smoke particulates in bigger heptane pool fires might due to the insufficient air

entrainment and subsequent mixing process with the fuel vapor. Compared with the plot of inclined radiative heat flux (Fig. 6), Figure 8 has a relatively narrow peak in the graph. It is anticipated that the deviations might come from the fact that the measured inclined radiative heat flux was the result of flame radiation perpendicular to the fuel surface. However, due to the radiation reflectivity and absorption (mainly by soot [43]), the farther the flame is away from the fuel surface, the less radiative heat flux will pass underneath the flame body to the fuel surface. This, to some extent, slows the changing rate of measured radiative heat flux as the normalized soot generation changes.

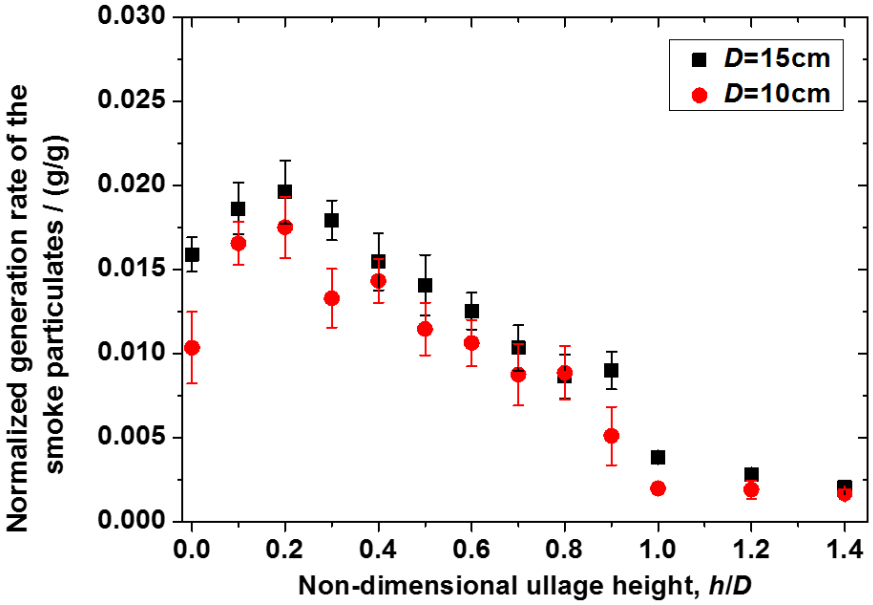

Fig. 8 Normalized generation rate of the smoke particulates vs. *h*/*D*.

Apart from the generation rate of the smoke particulates, the emission ratio of CO/CO_2 is another important parameter among the combustion emission products. The CO/CO_2 ratio is generally recognized as the indicator to evaluate the combustion completeness [44]. CO is a product of incomplete combustion. The higher the combustion completeness, the more CO will be burned into CO_2, resulting in a lower CO/CO_2 ratio. Figure 9 shows the ratio of CO/CO_2 with *h*/*D*. As illustrated in Fig. 9, the emission ratio of CO/CO_2 slightly increases with *h*/*D*, which means that the combustion completeness is reduced as the ullage height increases. And, more carbon of the fuel was transformed into CO due to the combustion incompleteness. For pool fires, significant air entrainment occurred around the primary anchoring zone [45]. The

increased ullage height will inhibit sufficient air entrained into the flame and mix with the fuel vapor, which causes the increase of incomplete combustion (CO/CO_2) and lower burning intensity. Besides, according to experimental observation, smoke particulates accumulated on the pool ullage wall due to its cooling effects on the plume combustion. As a result, the plume temperature was also affected, which we found that plume centerline temperature generally decreases with the ullage height [16].

Besides, it is known there is a positive correlation between CO emission rate and the soot yield for well-ventilated open burning [46, 47]. However, in the current study, the burning is confined by the ullage height. Then, there is a competition between the production of CO and soot for the oxidizer species -OH [48], which would result in the high emission of CO from sooting flames [49].

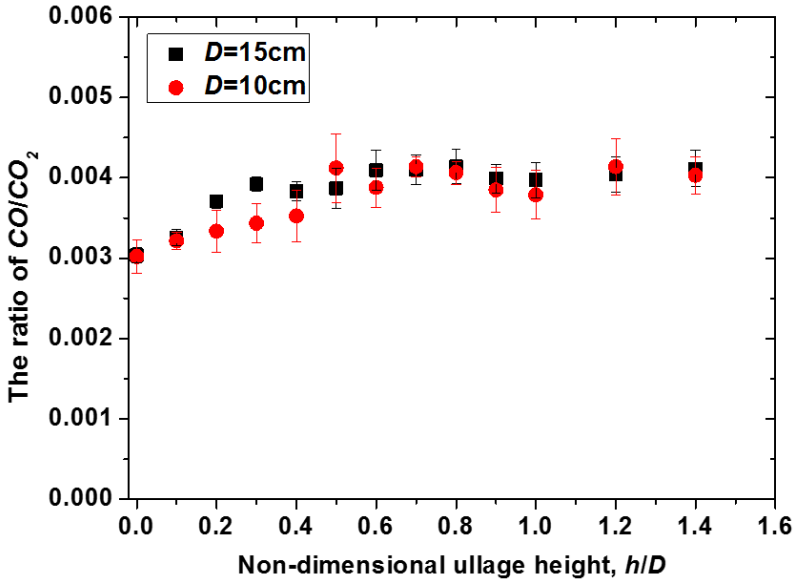

Fig. 9 The emission ratio of CO/ CO_2 vs. *h*/*D*.

To further quantitatively evaluate the effect of ullage height on the combustion completeness, the evolution of the combustion completeness with h/D is calculated based on the measured combustion emission products. The combustion completeness is the ratio of actual (or chemical) heat release rate with calculated ones, represented as,

$$\chi = Q / (m' H_c) \tag{13}$$

where H_c is the fuel combustion heat, Q is the actual heat release rate. Generally, there are two ways to calculate Q, one is based on the oxygen consumption method

(Eq. (14)) and the other is calculated on account of the CO and CO_2 generation (Eq. (15)). The latter method is more sensitive to lower heat release conditions [18], and is adopted in this study since the heat release rate is decreased to a very small value under higher ullage height conditions. We compared the calculated heat release rate of the above two methods and found that Q calculated by the oxygen consumption method was on average 36 % higher than that of the second method.

$$Q=\Delta H_{O_2}(m_{O_2,0}-m_{O_2}) \tag{14}$$

$$Q=(\Delta H_T/k_{CO_2})(m_{CO_2}\text{-}m_{CO_2,0})+[(\Delta H_T-\Delta H_{CO}k_{CO})/k_{CO}](m_{CO}\text{-}m_{CO,0}) \tag{15}$$

where ΔH_{O_2} is the averaged heat released when per unit mass of oxygen was consumed for complete combustion. Huggett [50] extensively tested a large number of fuels and obtained an averaged value for ΔH_{O_2} as 13.1 MJ·kg. $m_{O_2,0}$ and m_{O_2} are respectively the mass of O_2 before and during combustion. ΔH_T is the net heat of complete combustion, k_{CO_2} and k_{CO} are the stoichiometric yield of CO_2 and CO. ΔH_{CO} is the combustion heat of CO. m_{CO_2} and m_{CO} are the mass of CO_2 and CO during combustion. $m_{CO_2,0}$ and $m_{CO,0}$ are the mass of CO_2 and CO during combustion prior to ignition.

Figure 10 shows the relationship between the combustion completeness and *h*/*D*, and demonstrates that the combustion completeness generally decreases with *h*/*D*. The maximum combustion completeness reductions (between the zero and the maximum ullage height conditions) for the diameters of 10 cm and 15 cm pool fires are 18.4 % and 14.3 %, respectively.

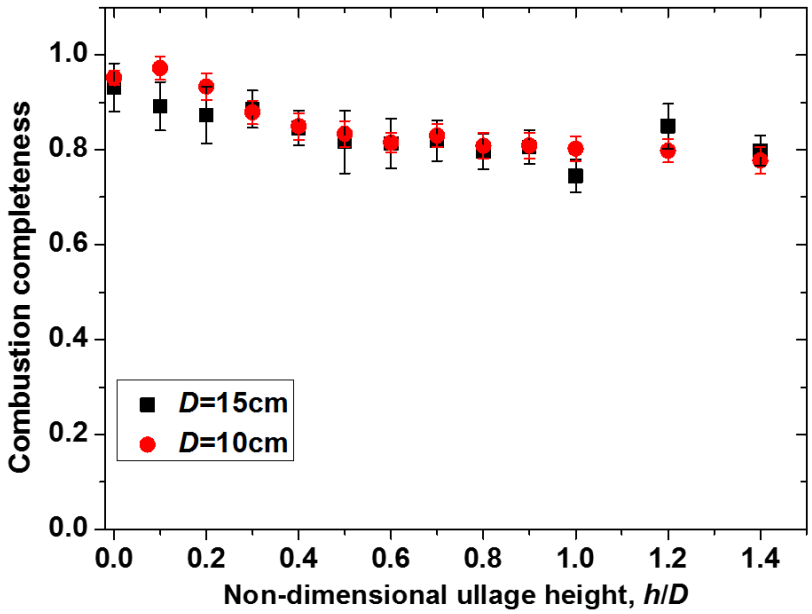

Fig. 10 Relationship between combustion completeness and *h*/*D*.

4. Conclusions

This paper presents the first effort to interpret the effects of ullage height on heat feedback and combustion mechanisms of heptane pool fires. Ullage height was set from zero to the value that flame self-extinguished. Flame shape, mass loss rate, temperatures of the pool sidewall and the liquid fuel, incident radiative heat flux on the fuel surface, and combustion emission products (smoke particulates, CO, CO_2) were recorded and analyzed. Major findings are summarized as follows.

(1) Ullage height has a significant effect on the flame shape. Under the influence of minor ullage height, the flame shape presents a rising mushroom cloud, with the unstable fire plume starting to form near the ullage upper rim. At large ullage height conditions, the flame behaves much stubbier and burns within the pool. And, the ambient air entrained into the pool from part of the pool mouth. After that, it mixes with the fuel vapor, and the fire plume leaves the pool from other parts of the pool mouth.

(2) With the increase of ullage height, the mass loss rate shows a decreasing trend. The temperature differences between the pool sidewall and the liquid fuel are almost unchanged. The increase of ullage height mainly restricts the air entrainment and mixing process between the air and the fuel vapor.

(3) The conductive heat feedback fraction increases with ullage height, and

conduction would be the dominant heat transfer mode when ullage height increases to a certain value. The incident radiative heat flux on the fuel surface is shown to first increase and then decrease with increasing ullage height. The evolution of radiative heat feedback fraction with ullage height is consistent with the incident radiative heat flux. This variation attributes to the restriction effect of ullage height, which will cause the changes of the soot volume fraction and the plume temperature. A reverse trend is found for the convective heat feedback fraction as ullage height increases. This is relevant to the development of turbulence intensities of the plume base.

(4) The profiles of the normalized generation rate of the smoke particulates well explain the evolutions of the incident radiative heat flux received by the fuel surface. The profiles of the CO/CO_2 ratio indicate that the combustion completeness decreases with ullage height. The maximum reductions of the combustion completeness are respectively 18.4 % and 14.3 % for the diameters of 10 cm and 15 cm heptane pool fires.

The current study reveals the effects of ullage height on heat feedback and combustion mechanisms of heptane pool fires. Reducing the heat received by the fuel would decrease the fuel gas evaporation rate, which results in the decreasing of fire growth and burning intensity of pool fires. Then, one practical finding of this study is that, for those pool fires with significant ullage height, it is reasonable to weaken the burning intensity and fire growth by cooling down the pool sidewall, as it transfers the dominant heat flux to the fuel. Based on accessible experimental resources, this work only applied: 1) a single radiometer placed on the center of the fuel surface to represent the averaged radiative heat feedback, 2) an experimental pool made of stainless-steel. Future work calls for: 1) conducting more detailed measurement of the radial radiative heat feedback along the fuel surface, 2) studying the effects of pool material (with different conductivity, radiation emissivity and reflectivity) on heat feedback mechanisms of pool fires, under different ullage heights.

Acknowledgements

This work was supported by National Natural Science Foundation of China (NSFC) under Grant No. 52036009, the Key Research and Development Program of Anhui Province under Grant No. 201903a05020024 and Anhui Provincial Natural Science Foundation under Grant No. 2008085UD07.

Appendix. Experimental error discussions

The uncertainties of the experimental parameters involved in this paper have been evaluated by adopting Moffat method [51, 52]. This method has been widely recognized and applied for quantitatively evaluating the uncertainties of heat transfer and flow related parameters [53, 54]. According to this method, the model uncertainty of is described by a root-sum-square (RSS) equation [51, 52],

$$\delta R = \left\{ (\frac{\partial R}{\partial x_1}\delta x_1)^2 + (\frac{\partial R}{\partial x_2}\delta x_2)^2 + ... + (\frac{\partial R}{\partial x_N}\delta x_N)^2 \right\}^{1/2} \tag{16}$$

where R is the function of N measured independent variables, $R = f(x_1, x_2..., x_N)$. In this paper, the measured independent variables include mass loss rate (m'), temperatures of the pool wall (T_w) and the fuel (T_l) and the incident radiative heat flux ($q_{rad.}$). $\delta x_i (i = 1, 2..., N)$ is the uncertainty of x_i . $\partial R / \partial x_i$ is the sensitivity coefficient representing the influence weight of x_i on *R*. Based on Eq. (16), the average relative uncertainties of the experimental and calculated parameters are shown in Table 2.

Table 2. Uncertainties of the measured and calculated parameters.

Parameters	Source of uncertainty	Average relative uncertainty
Mass loss rate, m'	Measurement	6.4 %
Temperature, T_w, T_l	Measurement	2.0 %, 1.7 %
Incident radiative heat flux, $q_{rad.}$	Measurement	7.0 %

Q_{fuel} calculated by Eq. (3)	m'	6.4 %
$Q_{rad.}$ calculated by Eq. (4)	$q_{rad.}$	6.4 %
$Q_{cond.}$ calculated by Eq. (5)	T_w, T_l	3.3 %
$\chi_{cond.}$ calculated by Eq. (8)	m', T_w, T_l	7.2 %
$\chi_{rad.}$ calculated by Eq. (8)	m', $q_{rad.}$	9.1 %
$\chi_{conv.}$ calculated by Eq. (8)	m', T_w, T_l, $q_{rad.}$	9.6 %
Normalized generation rate of the smoke particulates	V [18], Ω[55], m'	12.9 %
The ratio of CO/CO_2	Measurement [18]	1.4 %
Combustion completeness	Q [18], m'	12.7 %

References

[1] Klein R, Maevski I, Ko J, et al. Fuel pool development in tunnel and drainage as a means to mitigate tunnel fire size. Fire Safety Journal, 2018, 97: 87-95.

[2] Zhao G, Beji aT, Merci B. Study of FDS simulations of buoyant fire-induced smoke movement in a high-rise building stairwell. Fire Safety Journal, 2017, 91: 276-283.

[3] Drysdale D. An introduction to fire dynamics. John Wiley & Sons, 2011.

[4] Liu S, Studies on heat feedback and burning rate of pool fires under a horizontal air flow, Master Thesis, University of Science and Technology of China, China, 2011.

[5] Hamins A, Fischer S J, Kashiwagi T, et al. Heat feedback to the fuel surface in pool fires. Combustion Science and Technology, 1994, 97(1-3): 37-62.

[6] Nakakuki A. Heat transfer in small scale pool fires. Combustion and flame, 1994, 96(3): 311-324.

[7] Zhao J, Huang H, Jomaas G, et al. Experimental study of the burning behaviors of thin-layer pool fires. Combustion and Flame, 2018, 193: 327-334.

[8] Kuang C, Investigation into burning rate heat feedback mechanisms and radiation properties of pool fire in cross flow, Ph. D Thesis, University of Science and

Technology of China, China, 2019.

[9] Ge F, Simeoni A, Ji J, et al. Experimental study on the evolution of heat feedback in multiple pool fires. Proceedings of the Combustion Institute, 2021, 38(3): 4887-4895.

[10] Wan H, Yu L, Ji J. Experimental study on mass burning rate and heat feedback mechanism of pair of unequal circular pool fires of heptane. Proceedings of the Combustion Institute, 2021, 38(3): 4953-4961.

[11] Blinov V I, Khudyakov G N. Diffusion burning of liquids. Army Engineer Research and Development Labs Fort Belvoir VA, 1961.

[12] Orloff L. Simplified radiation modeling of pool fires, Symposium (International) on Combustion. Elsevier, 1981, 18(1): 549-561.

[13] Dlugogorski B Z, Wilson M. Effect of Ullage on Properties of Small-Scale Pool Fires. Developments in Chemical Engineering and Mineral Processing, 2000, 8(1-2): 149-166.

[14] Shi X, Sahu A K, Nair S, et al. Effect of ullage on burning behavior of small-scale pool fires in a cavity. Proceedings of the Combustion Institute, 2017, 36(2): 3113-3120.

[15] Liu C, Ding L, Jangi M, et al. Experimental study of the effect of ullage height on flame characteristics of pool fires. Combustion and Flame, 2020, 216: 245-255.

[16] Liu C, Ding L, Ji J. Experimental study of the effects of ullage height on fire plume centerline temperature with a new virtual origin model. Process Safety and Environmental Protection, 2021, 146: 961-967.

[17] Liu C, Jangi M, Ji J, et al. Experimental and numerical study of the effects of ullage height on plume flow and combustion characteristics of pool fires. Process Safety and Environmental Protection, 2021, 151: 208-221.

[18] ATME. 2058-00: standard test method for measurement of synthetic polymer material flammability using a fire propagation apparatus (FPA). Am Soc Test Mater, 2000;100.

[19] Jiao Y, Gao W, Liu N, et al. Interpretation on fire interaction mechanisms of

multiple pool fires. Proceedings of the Combustion Institute, 2019, 37(3): 3967-3974.

[20] Tao C, He Y, Li Y, et al. Effects of oblique air flow on burning rates of square ethanol pool fires. Journal of hazardous materials, 2013, (260): 552-562.

[21] Kong D, Zhang Z, Ping P, He X, et al. Effects of the initial fuel temperature on burning behavior of crude oil pool fire in ice cavities. Experimental Heat Transfer, 2018, 31(5): 436-449.

[22] Tian X, Liu C, Zhong M, et al. Experimental study and theoretical analysis on influencing factors of burning rate of methanol pool fire. Fuel, 2020, (269): 117467.

[23] Ma L, Nmira F, Consalvi J L. Large Eddy Simulation of medium-scale methanol pool fires-effects of pool boundary conditions. Combustion and Flame, 2020, 222: 336-354.

[24] Luketa A. Assessment of simulation predictions of hydrocarbon pool fire tests. SAND2010-2511, Sandia National Laboratories, Albuquerque, New Mexico, 2010, 87185.

[25] Cetegen B M, Ahmed T A. Experiments on the periodic instability of buoyant plumes and pool fires. Combustion and flame, 1993, 93(1-2): 157-184.

[26] Liu C, Wan H, Ji J, et al. Flame spread characteristics and a multi-cylinder radiation model for diesel tray fires against a sidewall. International Journal of Thermal Sciences, 2019, 139: 433-439.

[27] Fang J, Tu R, Guan J, et al. Influence of low air pressure on combustion characteristics and flame pulsation frequency of pool fires. Fuel, 2011, 90(8): 2760-2766.

[28] Weckman E J, Sobiesiak A. The oscillatory behaviour of medium-scale pool fires, Symposium (International) on Combustion. Elsevier, 1989, 22(1): 1299-1310.

[29] Rangwala A S. A novel experimental approach to enhance burning of oil-water emulsions by immersed objects. Department of Fire Protection Engineering, Worcester Polytechnic Institute, 2015.

[30] Fang J, Zheng S, Wang J, et al. An analysis of heat feedback effects of different

height embedded plates on promotion of pool fire burning using a variable B number. International Journal of Thermal Sciences, 2019, 145: 106041.

[31] Babrauskas V. Estimating large pool fire burning rates. Fire technology, 1983, 19(4): 251-261.

[32] A. Hamins, T. Kashiwagi, R.R. Buch, Characteristics of pool fire burning, Report No. ASTM STP 1284, Fire resistance of industrial fluids, 1996.

[33] Zhou Z, Wei Y, Li H, et al. Experimental analysis of low air pressure influences on fire plumes. International Journal of Heat and Mass Transfer, 2014, 70: 578-585.

[34] Raj V C, Prabhu S V. Measurement of geometric and radiative properties of heptane pool fires. Fire Safety Journal, 2018, 96: 13-26.

[35] Vali A, Nobes D S, Kostiuk L W. Fluid motion and energy transfer within burning liquid fuel pools of various thicknesses. Combustion and Flame, 2015, 162(4): 1477-1488.

[36] Hurley M J, Gottuk D T, Hall J R et al., SFPE Handbook of fire protection engineering, Springer, 2015.

[37] Persson H, Lönnermark A. Tank Fires-Review of fire incidents 1951-2003. 2004.

[38] Wang K, Fang J, Shah H R, et al. A theoretical and experimental study of extinguishing compressed air foam on an n-heptane storage tank fire with variable fuel thickness. Process Safety and Environmental Protection, 2020, 138: 117-129.

[39] Tewarson A, Jiang F H, Morikawa T, Ventilation-Controlled Combustion of Polymers. Combustion and Flame 95(1993):151–169.

[40] Brookes S J, Moss J B. Measurements of soot production and thermal radiation from confined turbulent jet diffusion flames of methane. Combustion and Flame, 1999, 116(1-2), 49-61.

[41] Kent, J H, Wagner, H G, Why do diffusion flames emit smoke. Combustion Science and Technology, 1984, 41: 245-269.

[42] Newman J S, Steciak J., Characterization of Particulates from Diffusion Flames. Combustion and Flame, 1984, 67: 55–64.

[43] Tien C L, Lee S C. Flame radiation. Progress in Energy and Combustion Science,

1982, 8(1): 41-59.

[44] Gottuk D T, Lattimer B Y, Effect of combustion conditions on species production, SFPE handbook of fire protection engineering. Springer, New York, NY, 2016: 486-528.

[45] Venkatesh S, Ito A, Saito K, et al. Flame base structure of small-scale pool fires, Symposium (International) on Combustion. Elsevier, 1996, 26(1): 1437-1443.

[46] Cheng L H, Yeh C F, Tsai K C, et al. Effect of pool fire scale of heavy fuel oil on the characteristics of PAH emissions. Fuel, 2019, 235: 933-943.

[47] Tewarson A, Khan M. Carbon monoxide and smoke emissions in fires. Interflam 2007, 1059-1069.

[48] Kliylii U O, Sivathanu Y R, Faeth G M. Carbon monoxide and soot emissions from buoyant turbulent diffusion flames. Fire Safety Science, 1991, 3: 625-634.

[49] Sen S, Puri I K. Thermal radiation modeling in flames and fires. Transport Phenonema in Fires, 2008: 301.

[50] Huggett C. Estimation of rate of heat release by means of oxygen consumption measurements. Fire and Materials, 1980, 4(2): 61-65.

[51] Moffat R J. Using uncertainty analysis in the planning of an experiment. 1985.

[52] Moffat R J. Describing the uncertainties in experimental results. Experimental Thermal and Fluid Science, 1988, 1(1): 3-17.

[53] Lelea D, Nishio S, Takano K. The experimental research on microtube heat transfer and fluid flow of distilled water. International Journal of Heat and Mass Transfer, 2004, 47(12-13): 2817-2830.

[54] Stasiek J, Collins M W, Ciofalo M, et al. Investigation of flow and heat transfer in corrugated passages—I. Experimental results. International Journal of Heat and Mass Transfer, 1996, 39(1): 149-164.

[55] Mulholland G W, Smoke Production and Properties, SFPE Handbook of Fire Protection Engineering, National Fire Protection Association, Quincy, MA, 2008.